CROATICA CHEMICA ACTA
CCACAA, ISSN 0011-1643, e-ISSN 1334-417X
Croat. Chem. Acta **87** (4) (2014) 307–314.
http://dx.doi.org/10.5562/cca2488

Feature Article

Intrinsic Properties of Nitric Oxide Binding to Ferrous and Ferric Hemes†

Barbara Chiavarino, Maria Elisa Crestoni, and Simonetta Fornarini*

Dipartimento di Chimica e Tecnologie del Farmaco, Università di Roma "La Sapienza", P. le A. Moro 5, I-00185, Roma, Italy

RECEIVED JUNE 3, 2014; REVISED SEPTEMBER 4, 2014; ACCEPTED SEPTEMBER 5, 2014

Abstract. Gas phase studies offer an ideal medium whereby structural and reactivity properties of charged species may be unveiled in the absence of solvent, matrix or counterion effects. In this environment NO binds to iron(II)- and iron(III)-hemes with comparable kinetics and equilibrium parameters, conclusively elucidating the factors determining the widely different affinity in protic solvents or in heme proteins. IRMPD spectroscopy of the isolated species provides unambiguous characterization of the gaseous nitrosyl heme complexes.

Keywords: five-coordinate hemes, nitrosyl complexes, FT-ICR mass spectrometry, IR spectroscopy, NO addition kinetics, metallobiomolecules

INTRODUCTION

In the past few decades inorganic, small molecules (NO, CO, H_2S), once considered primarily as toxic gases, have been discovered to be endogenously formed and to play an important role as signaling molecules.[1] For this reason, nitric oxide (nitrogen monoxide, NO) has gained the title of 'molecule of the year' by the journal Science in 1992.[2] Shortly afterwards, in 1998, the Nobel Prize in Medicine awarded to F. Murad, R. F. Furchgott and L. J. Ignarro has given worldwide recognition to the vast array of functions performed by this unique simple molecule.[3–5] Nitric oxide is in fact responsible for several physiological activities in mammalian biology. It is an important mediator in cell signaling, blood flow regulation and immune response. Because of its role in tumor growth and suppression, phototherapeutic processes and novel materials have been devised, aiming to release NO to biological targets.[6] The chemical interactions between nitric oxide and the biological targets are largely mediated by heme proteins. Heme proteins are involved as well in NO synthesis and elimination.[7–8] The binding of NO to the metal center of the heme prosthetic group is an essential part of the activation of this signaling molecule and this fact explains the significant effort addressed to directly characterize the structure, dynamics and reactivity of heme-NO complexes.[9–12] In this context we have become interested in studying the heme-NO interaction using the tools of gas-phase ion chemistry. The gaseous environment provides a medium where intrinsic structural and reactivity features of an ionic species may be highlighted in the absence of the manifold effects operating in solution. The significant information that can be obtained from isolating a charged species from counter ion, solvent or matrix, has been appreciated by Professor Mirjana Eckert-Maksic and taken advantage of in her seminal studies providing new insight into several aspects of physical organic chemistry.[13–19] In grateful recognition of the valuable contribution of a distinguished scientist and esteemed friend, we are dedicating an overview of our work on the heme-NO interaction focused on both reactivity and structural and spectroscopic issues.

NO Binding to Heme and Heme Proteins

Heme centers are involved in a large part of the biological activity of nitric oxide and mechanistic studies have elucidated the most significant features of NO binding to heme proteins. The heme enzymes and the related model complexes present largely different behavior depending on the metal oxidation state. Kinetic studies have been performed using a variety of experimental techniques and rate constants have been determined for the binding (k_f) and the release (k_r) of NO for a number of Fe^{II}- and Fe^{III}-heme proteins.[9–12] Exemplary data are

† Dedicated to Dr. Mirjana Eckert-Maksić on the occasion of her 70th birthday.

* Author to whom correspondence should be addressed. (E-mail: simonetta.fornarini@uniroma1.it)

summarized in Table 1.[9] Typically, the second order rate constants, k_f, are very high, on the order of 10^3 to 10^8 M^{-1} s^{-1} and also the equilibrium constants are quite high. Both kinetic and equilibrium constants are markedly higher when porphyrin/protein complexes holding iron(II) are involved. For example, the K value for nitric oxide binding to myoglobin, Mb(II), is 8 orders of magnitude higher than for metmyoglobin, Mb(III). It is well recognized that NO addition to hemes is a facile process when a very labile or vacant coordination site is available, which occurs in high spin iron(II) heme proteins.[10] Conversely, the iron(III) center in Mb(III) is six coordinate with imidazole and water occupying the axial positions. NO binding needs to be accompanied by release of a water molecule. Mechanistic studies evaluating the activation entropy and activation volume for NO addition support a limiting dissociative ligand substitution mechanism, as depicted in Equation (1) for an iron(III) porphyrin complex in aqueous solution.[11–12] Thus, one is drawn to the likely conclusion that in the heme protein the lability (or absence) of a leaving group, the accessibility of the heme and the characteristics of its surroundings are the important factors governing the dynamics of NO binding and release with biologically relevant metal centers. The nature of the metal appears to be the dominant factor rather than the free radical character of NO which behaves as other typical Lewis bases.

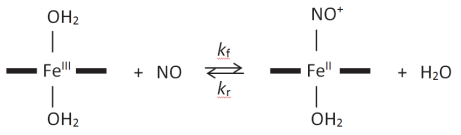

(1)

Aiming to disentangle the complex role of the heme environment, we decided to examine the neat interaction of NO with a heme center in an isolated state as provided by a low pressure gas phase. In this medium, the heme complex is in a well defined coordination state and is readily obtained as four coordinate at the metal center. A seminal study on the binding of NO to Fe^{III}-heme and to model Fe^{II}- and Fe^{III}-porphyrin complexes by Ridge and his coworkers has provided quantitative data on metalloporphyrin-NO bond strengths.[20] They used a variety of experimental approaches (radiative association, blackbody infrared radiative dissociation and association equilibria) unveiling the potential of gas phase ion chemistry in yielding valuable information on intrinsic properties of nitrosyl complexes performing important biological roles.

Table 1. Rate and equilibrium constants for NO binding to iron(II)/iron(III) porphyrin complexes and heme proteins[9]

Iron(II)/(III) porphyrin[(a)]	k_f / M^{-1} s^{-1}	k_r / s^{-1}	K / M^{-1}
Mb(II)	1.7×10^7	1.2×10^{-4}	1.4×10^{11}
Mb(III)	1.9×10^5	13.6	1.4×10^4
Hb(II)	2.5×10^7	4.6×10^{-5}	5.3×10^{11}
Hb(III)	4×10^3	1	4×10^3
Fe^{II}(TPPS)	1.8×10^9	≈ 0	$> 10^9$
Fe^{III}(TPPS)	7.2×10^5	6.8×10^2	1.1×10^3
Fe^{II}(TMPS)	1×10^9	–	–
Fe^{III}(TMPS)	3×10^6	7.3×10^2	4.1×10^3

[(a)] Mb: myoglobin; Hb: hemoglobin; TPPS: meso-tetra(4-sulfonatophenyl)porphyrinato dianion; TMPS: meso-tetra(sulfonatomesityl)porphyrinato dianion.

Formation of Charged Iron(II)- and Iron(III)-heme Ions in the Gas Phase

A simple access to iron(III) porphyrin complexes as singly charged, gaseous cations may be accomplished using electrospray ionization (ESI) of a solution of Fe^{III}(P)Cl.[21,22] The porphyrinato dianion, P, corresponds to removal of two central protons from the porphyrin macrocyle which may then act as tetradentate ligand for metal cations. Positively charged $[Fe^{III}(P)]^+$ species may thus be obtained by ESI, whereby the ions are delivered into the gas phase, void of any counterion and free from solvation. In this way, various P ligands may be examined, including protoporphyrin IX which releases the Fe^{III}-$heme^+$ ion. However, turning to iron(II) porphyrin complexes, Fe^{II}(P), they are now neutral and not amenable to be delivered and manipulated in the gas phase by mass spectrometric means. Forming negative ions of iron(II) heme by deprotonation of a propionic group (the straightforward choice) has never been successful by ESI in our experience. An alternative means for obtaining a charged iron(II) heme complex has been sought and found in the collision induced dissociation of microperoxidase (MP11, a heme undecapeptide derived from enzymatic cleavage of cytochrome c) ions. The m/z ratio corresponds to iron(II) heme b ion with an added hydrogen, so that the species may be conceived as a protonated iron(II) heme, Fe^{II}-$hemeH^+$. This novel complex has been thoroughly characterized both by its gas phase reactivity and by computations searching for plausible structures.[23]

By DFT calculations, the relative stability of various isomers holding the additional proton on different sites of the porphyrin ligand, on its substituents and on the metal atom itself has been assessed. The most stable isomer is the one corresponding to protonation on one of the peripheral vinyl groups and the optimized structure is shown in Figure 1. All other isomers are higher in energy by more than 55 kJ mol^{-1}. The computational results have also allowed an analysis of the spin density distribution. In the most stable protonated isomer, the spin density distribution displays an excess of α spin at

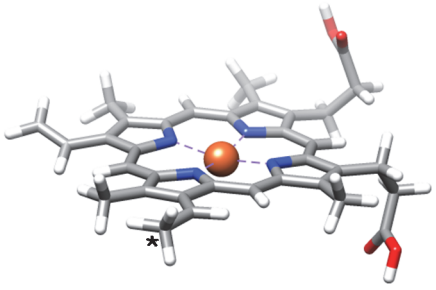

Figure 1. Optimized structure for Fe^{II}-$hemeH^+$ ions. The protonated carbon on the peripheral vinyl group is indicated by an asterisk.

the iron atom and excess β spin on the carbon atom of the protonated vinyl group directly linked to the tetrapyrrole macrocycle. Thus the CH_3CH– group acquires radical character which may be depicted as a consequence of electron transfer from Fe^{II} to the protonated porphyrin system. The charge transfer is partial so that the species may be envisioned as corresponding to an intermediate situation between Fe^{II}-$hemeH^+$ and $[Fe^{III}$-$heme H^{\cdot}]^+$ formal descriptions.

Ion-molecule Reactions to Characterize Gaseous Iron(II)- and Iron(III)-heme Ions

Ion-molecule reactions are increasingly recognized as analytical and structurally diagnostic tool.[24] Fourier transform ion cyclotron resonance (FT-ICR) mass spectrometry has provided the instrumental basis to characterize the reactivity and thermodynamic features of iron(II)- and iron(III)-heme ions. The ions of interest, generated by ESI, are conveyed into the FT-ICR cell where they are allowed to react with a stationary concentration of a selected neutral.

H/D-exchange reactions are a useful probe of ionic structures. Fe^{II}-$hemeH^+$ ions have been assayed by testing their reactivity towards D_2O, CD_3CO_2D, and ND_3 as exchange reagents and comparing their behavior with the one displayed by Fe^{III}-$heme^+$ ions.[23] Both ions are unreactive towards D_2O while the exchange reactivity with CD_3CO_2D displayed by Fe^{II}-$hemeH^+$ is similar to the one shown by Fe^{III}-$heme^+$, both for the number of labile hydrogens, only two, and for the rate constant values, differing by less than a factor of two. The gained evidence indicates that the labile hydrogens pertain to the propionyl substituents at the periphery of the protoporphyrin IX. Being remote from the metal center, their reactivity is not appreciably different. A ligand association reaction is then more likely to point out any difference in reactivity behavior that may depend on the metal oxidation state.

Table 2. Kinetic data for ligand (L) association reactions of heme cations[23]

Ligand	k_f[(a)] for Fe^{III}-$heme^+$	k_f[(a)] for Fe^{II}-$heme^+$
CH_3CO_2H	0.07	–
NH_3	0.34	–
NO	0.22	0.33
$(C_2H_5O)_3P$	13.0	4.0

[(a)] Second order rate constant for the ligand addition reaction, in units of 10^{-10} cm^3 $molecule^{-1}$ s^{-1}, at 300 K.

Sample kinetic data are listed in Table 2 summarizing the rate constants for ligand addition to Fe^{III}-$heme^+$ or Fe^{II}-$hemeH^+$ ions. The collected data show that the ion chemistry of Fe^{II}-$hemeH^+$ ions presents notable differences with respect to the one displayed by Fe^{III}-$heme^+$. Lewis bases, such as acetic acid, ammonia and triethylphosphite, are distinctly less reactive with Fe^{II}-$hemeH^+$ ions. In the comparison, $(C_2H_5O)_3P$ is the least disfavored ligand, in agreement with its soft character ensuring enhanced affinity for iron(II) with respect to iron(III). This relative reactivity order, however, is inverted in the reaction with NO. This finding is in line with the expectations for a heme holding a metal with iron(II) character. Somewhat surprisingly, the reactivity Fe^{III}-$heme^+$ or Fe^{II}-$hemeH^+$ ions with NO is quite comparable and this reaction has become the focus of deepened effort to obtain complete reactivity and thermodynamic data.

Kinetic and Thermodynamic Parameters for NO Binding to Iron(II)- and Iron(III)-heme Ions

In order to assess kinetic and equilibrium data for the NO addition reaction, different experimental procedures have been exploited. In the study of association reactions either the reactant ion or the formed ion-neutral complex may be isolated and their reaction kinetics evaluated at varying neutral pressure. In this way the rate constants for the forward and reverse reaction (k_f and k_r, respectively) may be evaluated (Equation 2, where M^+ is either Fe^{III}-$heme^+$ or Fe^{II}-$hemeH^+$).[23,25] Their ratio, yielding the reaction equilibrium constant, has been compared with the equilibrium constant value derived from the steady ion abundance ratio observed at long reaction time, the two values nicely matching each other. Exemplary kinetic plots are shown in Figure 2. In the case of Fe^{II}-$hemeH^+$ ions, highly basic ligands such as $(CH_3)_2NH$, pyridine or $(CH_3O)_3PO$ do form adduct ions, although the reaction does not go to completion. In contrast, other tested ligands, including the one of major interest in the present study, namely NO, react with Fe^{II}-$hemeH^+$ leading to complete conversion of the free ion into Fe^{II}-$hemeH(L)^+$, thereby hampering a determination of the equilibrium constant by direct evaluation of the relative free and adduct ion abundances.

$$M^+ + L \underset{k_r}{\overset{k_f}{\rightleftharpoons}} ML^+ \qquad (2)$$

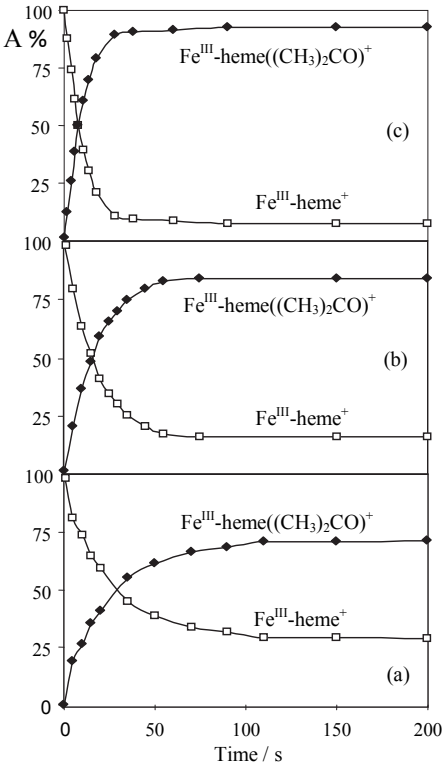

Figure 2. Kinetic plots for the Fe^{III}-heme$^+$ ion reaction with acetone at (a) 5.2 × 10^{-8} mbar; (b) 8.7 × 10^{-8} mbar; (c) 2.1 × 10^{-7} mbar.

The equilibrium constant for heme cation binding to strongly bound ligands, namely the *K* value for reaction 2, may however be obtained from a study of ligand exchange reactions as illustrated in Equation 3 (where M$^+$ is either Fe^{III}-heme$^+$ or Fe^{II}-hemeH$^+$). Ligand transfer equilibria, characterized by relatively modest free energy changes, are routinely accessible to FT-ICR mass spectrometry and lend themselves to build a ladder of increasing thermodynamic drive for ligand binding to iron(II) / (III) hemes. The scope may thus be reached of connecting the least bound and the most effective ligand. In this way one can obtain quantitative thermodynamic data for the association of NO to iron(II) / (III) hemes.

$$M(L_1)^+ + L_2 \overset{K}{\rightleftharpoons} L_1 + M(L_2)^+ \qquad (3)$$

The relative $\Delta G_3°$ for ligand transfer equilibria (Equation 3), organized in the framework of a ladder, is depicted in Figure 3 for the ligand addition to Fe^{III}-heme$^+$ ions.[25] The listed ligands were chosen to represent the various functionalities that are present in a protein backbone. One may note, for example, that the equilibrium for addition of acetone, illustrated in Figure 2, yields $\Delta G_2°$(binding) = −14.6 kcal mol^{-1} (Equation 2). This value, combined with $\Delta G_3°$ =

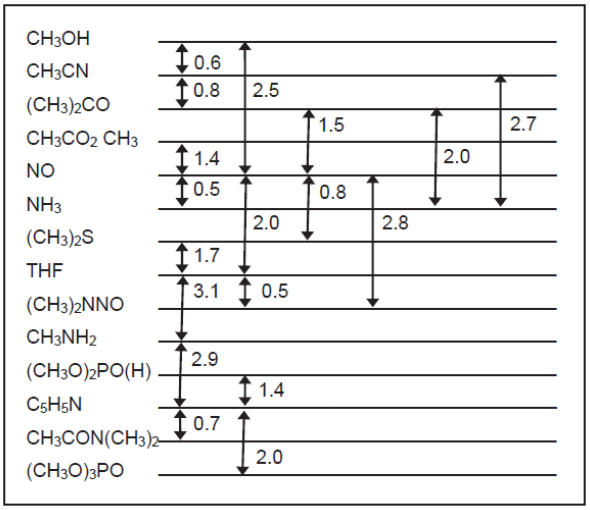

Figure 3. $\Delta G_3°$ (kcal mol^{-1}, 300 K) ladder for the Fe^{III}-heme$^+$ transfer reactions between selected pairs of ligands.

−1.5 kcal mol^{-1} for acetone / NO ligand transfer gives $\Delta G_2°$= −16.1 kcal mol^{-1} for NO binding to Fe^{III}-heme$^+$ ions. In general, it is found that $-\Delta G_2°$ values for heme cation binding, measuring the thermodynamic drive toward association of the sampled ligand, display a relationship with the gas phase basicity for the proton (GB). In other words, the most basic ligands are the ones which bind both Fe^{III}-heme$^+$ and Fe^{II}-hemeH$^+$ ions more tightly.[23,25] This behavior is illustrated in Figure 4, where a linear correlation is drawn between -$\Delta G_2°$ for ligand binding to Fe^{III}-heme$^+$ and the GB of the ligand. Remarkably, however, NO shows quite a distinct behavior when compared to other sampled molecules. The pertaining $-\Delta G_2°$ value equal to 16.1 kcal mol^{-1} is exceptionally high if compared with a GB value of only 121 kcal mol^{-1}.

Remarkable properties towards NO binding are common to both Fe^{III}-heme$^+$ and Fe^{II}-hemeH$^+$ ions. Using the described tools and procedures, kinetic and thermodynamic parameters for NO binding are obtained

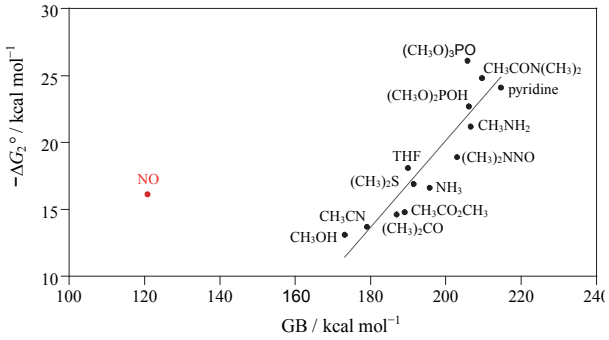

Figure 4. General correlation between the ligand binding free energy ($-\Delta G_2°$) to Fe^{III}-heme$^+$ cation plotted versus the gas phase basicity (GB) of the ligand toward the proton.

Table 3. Kinetic and equilibrium data for NO binding to gaseous iron (II/III) heme ions at 300 K[26]

Reactant ion	k_f / 10^{-11} cm^3 molecule^{-1} s^{-1}	k_r / 10^{-3} s^{-1}	K / 10^{11} atm^{-1}
Fe^{III}-heme$^+$	2.2	0.9	5.3
Fe^{II}-hemeH$^+$	3.3	0.8	5.7

and collected in Table 3.[26] In this way a comprehensive picture of the kinetics and equilibrium data is presented regarding the elementary process of NO addition to four-coordinate Fe^{II}- or Fe^{III}-heme ions. Not only is NO an exceptional ligand towards heme ions in the well defined four coordination state, it also shows strikingly similar values for the binding free energies and so-derived equilibrium constants to either Fe^{III}-heme$^+$ and Fe^{II}-hemeH$^+$ ions.

The rate constants are also comparable, pointing to a unified pattern whereby four coordinate iron (II / III) heme ions bind NO with closely similar kinetic and thermodynamic parameters in their gas phase reaction at 300 K. No indication has ever been obtained for the formation of six-coordinate dinitrosyl complexes under the prevailing experimental conditions.

Computational Survey of NO Binding Energies to Iron(II)- and Iron(III)-heme Ions

Density functional theory (DFT) based methods, a computational approach suited for sizeable organometallic systems,[27,28] have been exploited to estimate the NO binding energies to either Fe^{III}-heme$^+$ or Fe^{II}-hemeH$^+$ ions in five coordinate, gaseous complexes.[26] An intermediate spin state, namely quartet and triplet, is recognized to be the ground state for iron(III)- and iron(II)-porphyrins, respectively. The reaction with NO, a strong field ligand, yields low spin, singlet and doublet, nitrosyl complexes from Fe^{III}-heme$^+$ or Fe^{II}-hemeH$^+$ ions, respectively. The optimized geometries of [Fe^{III}-heme(NO)]$^+$ and [Fe^{II}-hemeH(NO)]$^+$ ions are shown in Figure 5. In both complexes NO is attached in the η^1-NO configuration. The geometry of [Fe^{III}-heme(NO)]$^+$ is characterized by Fe–N and N–O bond distances of 1.61 and 1.17 Å, respectively, by an upward displacement of iron relative to the porphyrin nitrogens equal to 0.36 Å and by a Fe–N–O angle of 178.6°. In the case of [Fe^{II}-hemeH(NO)]$^+$, the upward displacement of iron is 0.25 Å, Fe–N and N–O bond distances are 1.71 and 1.18 Å, respectively, and the Fe–N–O angle is 145.6°. The binding energy of [Fe^{III}-heme(NO)]$^+$ is 34.4 kcal mol^{-1} with respect to quartet Fe^{III}-heme$^+$ and ^{2}NO, while a value of 33.5 kcal mol^{-1} is obtained for [Fe^{II}-hemeH(NO)]$^+$ relative to dissociation into triplet [Fe^{II}-hemeH]$^+$ and ^{2}NO. These values indicate a quite comparable binding energy for NO addition to either Fe^{III}-heme$^+$ or Fe^{II}-hemeH$^+$ ions and are in full agreement with the experimental findings regarding the NO association equilibria to naked iron(II)- and iron(III)-heme ions.[26]

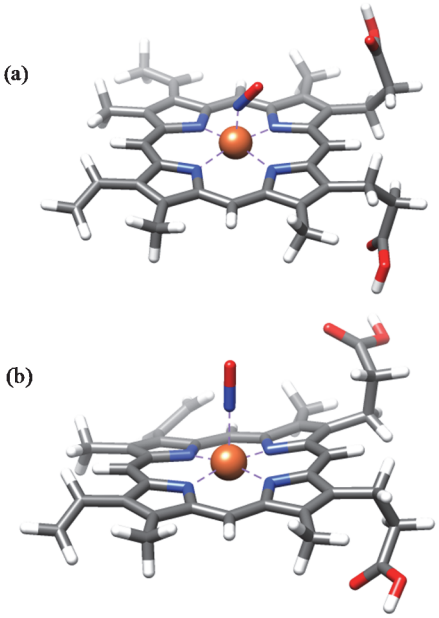

Figure 5. Structures of (a) [Fe^{II}-hemeH(NO)]$^+$ and (b) [Fe^{III}-heme(NO)]$^+$.

Intrinsic Properties for NO Addition to Iron(II)- and Iron(III)-heme Ions

Assessing the intrinsic properties for NO addition to ferrous and ferric heme is a particularly demanding task when dealing with these species in solution or even in a protein environment. As stated in the introductory paragraphs the reactivity behavior of iron(II)- and iron(III)-hemes and heme proteins are markedly different. The difference has been ascribed to the requirement of either a very labile or a vacant coordination site on iron for a facile addition of NO to occur. This condition is met in high spin iron(II)-heme proteins which show also the largest values for the association equilibrium constants. In contrast, iron(III)-heme proteins and model complexes have revealed large and positive activation entropies and activation volumes consistent with a dissociative ligand substitution mechanism for both NO binding and release.[12] In the gas phase, we face iron(II)- and iron(III)-heme ions that are both four coordinate at the metal core. The metal center presents exactly the same environment and any difference in kinetics and equilibrium data is therefore a consequence of the different oxidation state and electronic structure. However, this difference in iron(II)- and iron(III)-heme ions apparently does not cause an effect in the relative kinetic and thermodynamic data for the NO addition reaction. In the gas phase the nitrosylation reaction involves a neat bond formation process bearing just the consequence of spin

change along the reaction. Fortuitously, the observed results yield quite comparable kinetics and equilibrium constants for the formation of both $[Fe^{III}\text{-heme(NO)}]^+$ and $[Fe^{II}\text{-hemeH(NO)}]^+$ ions. However, a careful characterization of the so-formed nitrosyl complexes is desirable in order to precisely confirm the assigned electronic difference.

Vibrational Signatures of NO Binding to Iron(II)- and Iron(III)-heme Ions

IR spectroscopy is a key technique to study heme-nitrosyl complexes because the vibrational properties of these complexes are very sensitive to the spin state, the oxidation state and the molecular geometry of the metal atom.[29–31] In particular, the ν(NO) stretching mode presents characteristic frequencies and usually pronounced activity. Furthermore, it may be easily identified because of the distinct redshift upon isotopic substitution from ^{14}NO to ^{15}NO. Vibrational spectroscopy of gaseous charged species has become a viable spectroscopic tool only recently, owing to the development of infrared multiple photon dissociation (IRMPD) spectroscopy.[32] The employed instrumental setup is based on the coupling of a laser source of high fluence and tunability with a FT-ICR or quadrupole ion trap mass spectrometer. The laser light shined on the sampled ion leads to multiple photon absorption when the frequency is resonant with an active vibrational mode, heating the ion up to the dissociation threshold. The photofragmentation yield reported as a function of the laser radiation provides information on the IR spectrum of the sampled species. The methodology has been successfully adopted to characterize a variety of gaseous, ionic species, providing information hardly accessible by other means.[33–42] Both $[Fe^{III}\text{-heme(NO)}]^+$ and $[Fe^{II}\text{-hemeH(NO)}]^+$ ions have been assayed by IRMPD spectroscopy. The sampled ions have been obtained as usual by allowing the Fe^{III}-heme$^+$ or Fe^{II}-hemeH$^+$ precursors to react with a stationary concentration of NO prior to selection and trapping in the FT-ICR cell. Five coordinate nitrosyl complexes are thus formed under strictly comparable and controlled conditions. The observed photofragmentation process when the IR frequency matches the frequency of an IR active vibration involves the loss of NO from both $[Fe^{III}\text{-heme(NO)}]^+$ and $[Fe^{II}\text{-hemeH(NO)}]^+$ ions. The IRMPD spectra, bearing a direct relationship with the linear IR spectrum of the sampled species,[32] have been recorded in the structurally diagnostic 'fingerprint' region and are displayed in Figure 6.[43,44] Extensive portions of the spectra are very similar, as expected from the close similarity of the two complexes. For example, the 1000−1220 cm^{-1} range, encompassing porphyrin deformation modes, presents matching features. A similar pronounced band at *ca*. 1260 cm^{-1} is due to C–OH stretching and COH in plane bending vibrations in the spectra of both species. A distinct difference appears in the 1600−1900 cm^{-1} range, characterized by the presence of two prominent bands expected to arise from C=O and NO stretching modes. The ^{15}NO-labelled complexes display a significant redshift of ca. 30 cm^{-1} for the band at 1842 cm^{-1} in the spectrum of $[Fe^{III}\text{-heme(NO)}]^+$ (shifted to *ca*. 1810 cm^{-1}) and for the absorption at 1720 cm^{-1} in the spectrum of $[Fe^{II}\text{-hemeH(NO)}]^+$ (shifted to *ca*. 1694 cm^{-1}).[43,44] A red shift of about 30 cm^{-1} is indeed consistent with an oscillator involving N−O bond stretching upon substitution of ^{14}N with ^{15}N. In the two IRMPD spectra the second strong absorption in the 1600−1900 cm^{-1} range, which is observed at *ca*. 1750 cm^{-1}, maintains its frequency constant with the ^{15}N / ^{14}N isotope change and is therefore assigned to the C=O stretching mode of the propionic acid functionalities on the porphyrin periphery. The N−O stretching frequency in naked, five coordinate $[Fe^{III}\text{-heme(NO)}]^+$ and $[Fe^{II}\text{-hemeH(NO)}]^+$ complexes is then 1842 cm^{-1} and 1720 cm^{-1}, respectively. In a very recent paper the ν(NO) stretching frequency of 1660 cm^{-1} has been reported for a five-coordinate nitrosyliron(II) complex, Fe(Porph)(NO), where Porph is the dianion of protoporphyrin IX dimethyl ester, sampled by IR spectroscopy in KBr pellet.[31] While this frequency is significantly lower than the one pertaining to the gaseous complex, it is interesting to notice that the ν(CO) stretching frequency of Fe(Porph)(NO) in KBr is 1740 cm^{-1}, almost unaffected for the somewhat different species in the markedly different environment.

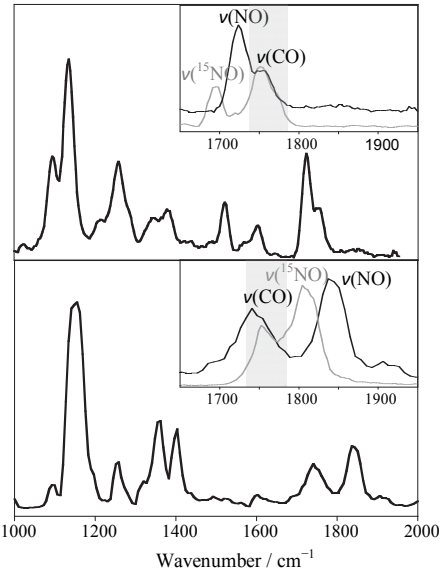

Figure 6. IRMPD spectra of (a) $[Fe^{II}\text{-hemeH(NO)}]^+$ and (b) $[Fe^{III}\text{-heme(NO)}]^+$. In both panels the insert illustrates an enlarged portion of the spectrum in the 1650−1950 cm^{-1} range. The spectra of the ^{15}NO-labelled species, showing the red shift of ν(NO), are drawn in gray.

The relatively low value of ν(NO) may be qualitatively accounted for by the contribution of a $Fe^{III}NO^-$ resonance structure, conveying significant π^* electron density on the nitrosyl group.

Turning to iron(III) nitrosyl complexes, the observed ν(NO) stretching frequency of 1842 cm^{-1} for naked $[Fe^{III}$-heme(NO)$]^+$ falls close to the nitrosyl absorption at 1838 cm^{-1} reported for $Fe^{III}(OEP)(NO)^+ClO_4^-$, where OEP is the dianion of octaethylporphyrin, in the solid state.[45] In this latter five coordinate iron porphyrin nitrosyl complex, however, ν(NO) depends on the crystalline form and on the presence of a solvent molecule and the complex is prone to interact with the counterion and to form π–π interacting dimers. The ν(NO) value for unperturbed five-coordinate nitrosyl iron(III) porphyrin complexes is however sensitive to the porphyrin peripheral substituents. In fact, in the gaseous model complexes $[Fe^{III}(TPP)(NO)]^+$ and $[Fe^{III}(TPFPP)(NO)]^+$, where TPP is the dianion of 5,10,15,20-tetrakis-phenyl-porphyrin and TPFPP is the dianion of 5,10,15,20-tetrakis-pentafluorophenyl-porphyrin, the NO stretching frequency is observed at 1825 and 1859 cm^{-1}, respectively.[46] The two complexes share a similar structure and a common singlet $^1A_1$ ground electronic state, yet present different electronic effect of the four meso substituents, allowing a comparison of the consequences caused by the phenyl versus pentafluorophenyl substitution.

It is interesting to mention here about a recent report on the ferric heme nitrosyl complex, $[Fe^{III}$-heme(NO)$]^+$, assayed in the gas phase by UV photodissociation spectroscopy in the Soret band region.[47] The Soret band is found to be blue shifted compared to naked ferric heme. This finding points once again to a distinct behavior relative to NO ligation within a heme protein, typically displaying a red rather than a blue shift. In contrast, the absorption of $[Fe^{III}$-heme(NO)$]^+$ in the Q band region is found to be redshifted relative to isolated Fe^{III}-heme$^+$ and similar to that of ferric heme nitrosyl proteins, pointing to a negligible perturbation by the microenvironment.[48]

The role environmental factors are playing in each case clearly deserves further investigation.

CONCLUSION

The comparative examination of the kinetics and thermodynamic parameters for the association reaction of iron(II)- and iron(III) heme ions to NO has been thoroughly investigated in the gas phase and the major results are reported in the present feature article. Standard mass spectrometric techniques such as FT-ICR mass spectrometry have provided the tools to unveil the intrinsic reactivity behavior of iron(II)- and iron(III) heme ions, namely the prosthetic groups that perform important biological functions in heme proteins. The kinetic and thermodynamic data characterizing these systems in the dilute gas phase are unaffected by external factors due to the presence of solvent, counterions, protein matrix, π–π aggregates, and axial ligands. The distinction between ferrous and ferric heme is clear in the different reactivity with the whole set of tested ligands (with the exception of NO) and is confirmed by the different spectroscopic properties of the two nitrosyl complexes. In the gas phase, Fe^{III}-heme$^+$ or Fe^{II}-hemeH$^+$ ions display quite comparable rate and equilibrium constants for NO addition. This finding is in marked contrast with a range in forward rate constant values spanning more than eight orders of magnitude for Fe^{III}- and Fe^{II}-heme proteins.[10] It has been recognized that in protic solvents ferric hemes undergo NO addition by a mechanism dominated by solvent ligand dissociation. Clearly, the gas phase offers a valuable advantage in allowing the heme ions to be examined under strictly equal coordination environment. In concert with experiment, DFT calculations have been undertaken to provide an independent source for the NO binding energies, confirming approximately equal values for both Fe^{III}-heme$^+$ and Fe^{II}-hemeH$^+$ ions. Finally, the structural and vibrational features of the two exemplary ions have been assayed by IRMPD spectroscopy. The IR spectra reflect the nature of the binding between NO and iron and display characteristically higher NO stretching frequency for the iron(III)- relative to the iron(II)-heme complex.

REFERENCES

1. J. M. Fukuto, S. J. Carrington, D. J. Tantillo, J. G. Harrison, L. J. Ignarro, B. A. Freeman, A. Chen, and D. A. Wink, *Chem. Res. Toxicol.* **25** (2012) 769–793.
2. E. Culotta and D. E. Koshland, *Science* **258** (1992) 1862−1865.
3. F. Murad, *Angew. Chem. Int. Ed.* **38** (1999) 1856−1868.
4. R. F. Furchgott, *Angew. Chem. Int. Ed.* **38** (1999) 1870−1880.
5. L. J. Ignarro, *Angew. Chem. Int. Ed.* **38** (1999) 1882−1892.
6. P. T. Burks, J. V. Garcia, I. R. Gonzalez, J. T. Tillman, M. Niu, A. A. Mikhailovsky, J. Zhang, F. Zhang, and P. C. Ford, *J. Am. Chem. Soc.* **135** (2013) 18145−18152.
7. H. M. Abu-Soud, K. Ichimori, H. Nakazawa, and D. J. Stuehr, *Biochemistry* **40** (2001) 6876−6881.
8. A. R. Hurshman and M. A. Marletta, *Biochemistry* **34** (1995) 5627−5634.
9. A. Wanat, M. Wolak, L. Orzel, M. Brindell, R. van Eldik, and G. Stochel, *Coord. Chem. Rev.* **229** (2002) 37−49.
10. M. Hoshino, L. Laverman, and P. C. Ford, *Coord. Chem. Rev.* **187** (1999) 75−102.
11. W. Macyk, A. Franke, and G. Stochel, *Coord. Chem. Rev.* **249** (2005) 2437–2457.
12. I. Ivanovic-Burmazovic and R. van Eldik, *Dalton Trans.* **39** (2008) 5259−5275.
13. Z. Glasovac, V. Strukil, M. Eckert-Maksic, D. Schroder, M. Schlangen, and H. Schwarz, *Int. J. Mass Spectrom.* **290** (2010) 22−31.
14. A. Tintaru, J. Roithova, D. Schroder, L. Charles, I. Jusinski, Z.

Glasovac, and M. J. Eckert-Maksic, *Phys. Chem. A* **112** (2008) 12097−12103.
15. Z. Glasovac, V. Strukil, M. Eckert-Maksic, D. Schroeder, M. Kaczorowska, and H. Schwarz, *Int. J. Mass Spectrom.* **270** (2008) 39−46.
16. I. Antol, Z. Glasovac, M. C. Hare, M. Eckert-Maksic, and S. R. Kass, *Int. J. Mass Spectrom.* **222** (2003) 11−26.
17. Z. Glasovac, M. Eckert-Maksic, J. E. Dacres, and S. R. Kass, *J. Chem. Soc., Perkin Trans.* **2** (2002) 410−415.
18. Z. Glasovac, M. Eckert-Maksic, K. M. Broadus, M. C. Hare, and S. R. Kass, *J. Org. Chem.* **65** (2000) 1818−1824.
19. L. Moore, R. Lubinski, M. C. Baschky, G. D. Dahlke, M. Hare, T. Arrowood, Z. Glasovac, M. Eckert-Maksic, and S. R. Kass, *J. Org. Chem.* **62** (1997) 7390−7396.
20. O. Chen, S. Groh, A. Liechty, and D. P. Ridge, *J. Am. Chem. Soc.* **121** (1999) 11910−11911.
21. L. A. Hayes, A. M. Chappell, E. E. Jellen, and V. Ryzhov, *Int. J. Mass Spectrom.* **227** (2003) 111−120.
22. T. Gozet, L. Huynh, and D. K. Bohme, *Int. J. Mass Spectrom.* **279** (2009) 113−118.
23. B. Chiavarino, M. E. Crestoni, S. Fornarini, and C. Rovira, *Chem. Eur. J.* **13** (2007) 776−785.
24. S. Osburn and V. Ryzhov, *Anal. Chem.* **85** (2013) 769−778.
25. F. Angelelli, B. Chiavarino, M. E. Crestoni, and S. Fornarini, *J. Am. Soc. Mass Spectrom.* **16** (2005) 589−598.
26. B. Chiavarino, M. E. Crestoni, S. Fornarini, and C. Rovira, *Inorg. Chem.* **47** (2008) 7792−7801.
27. E. M. Siegbahn and T. Borowski, *Acc. Chem. Res.* **39** (2006) 729−738.
28. A. Ghosh, *J. Biol. Inorg. Chem.* **11** (2006) 712−724.
29. L. E. Goodrich, F. Paulat, V. K. K. Praneeth, and N. Lehnert, *Inorg. Chem.* **49** (2010) 6293−6316.
30. W. R. Scheidt, A. Barabanschikov, J. W. Pavlik, N. J. Silvernail, and J. T. Sage, *Inorg. Chem.* **49** (2010) 6240−6252.
31. G. R. A. Wyllie, N. J. Silvernail, A. G. Oliver, C. E. Schulz, and W. R. Scheidt, *Inorg. Chem.* **53** (2014) 3763−3768.
32. J. Oomens, B. G. Sartakov, G. Meijer, and G. von Helden, *Int. J. Mass Spectrom.* **254** (2006) 1−19.
33. F. Lanucara, B. Chiavarino, D. Scuderi, P. Maitre, S. Fornarini, and M. E. Crestoni, *Chem. Commun.* **50** (2014) 3845−3848.
34. B. Chiavarino, M. E. Crestoni, S. Fornarini, J. Lemaire, L. Mac Aleese, and P. Maître, *ChemPhysChem* **6** (2005) 437−440.
35. A. De Petris, A. Ciavardini, C. Coletti, N. Re, B. Chiavarino, M. E. Crestoni, and S. Fornarini, *J. Phys. Chem. Lett.* **4** (2013) 3631−3635.
36. B. Chiavarino, P. Maitre, S. Fornarini, and M. E. Crestoni, *J. Am. Soc. Mass Spectrom.* **24** (2013) 1603−1607.
37. F. Lanucara, M. E. Crestoni, B. Chiavarino, S. Fornarini, O. Hernandez, D. Scuderi, and P. Maitre, *RSC Adv.* **3** (2013) 12711−12720.
38. M.E. Crestoni, B. Chiavarino, D. Scuderi, A. Di Marzio, and S. Fornarini, *J. Phys. Chem. B* **116** (2012) 8771−8779.
39. B. Chiavarino, M. E. Crestoni, S. Fornarini, S. Taioli, I. Mancini, and P. Tosi, *J. Chem. Phys.* **137** (2012) 024307.
40. F. Lanucara, B. Chiavarino, S. Fornarini, and M. E. Crestoni, *Chem. Phys. Lett.* **588** (2013) 215−219.
41. F. Lanucara, B. Chiavarino, M. E. Crestoni, D. Scuderi, R. K. Sinha, P. Maître, and S. Fornarini, Int. J. Mass Spectrom. **330−332** (2012) 160−167.
42. B. Chiavarino, M. E. Crestoni, J. Lemaire, P. Maitre, and S. Fornarini, *J. Chem. Phys.* **139** (2013) 071102.
43. B. Chiavarino, M. E. Crestoni, S. Fornarini, F. Lanucara, J. Lemaire, P. Maitre, and D. Scuderi, *ChemPhysChem* **9** (2008) 826−828.
44. F. Lanucara, D. Scuderi, B. Chiavarino, S. Fornarini, P. Maitre, and M. E. Crestoni, *J. Phys. Chem. Lett.* **4** (2013) 2414−2417.
45. D. P. Linder, K. R. Rodgers, J. Banister, G. R. A. Wyllie, M. K. Ellison, and W. R. Scheidt, *J. Am. Chem. Soc.* **126** (2004) 14136−14148.
46. F. Lanucara, B. Chiavarino, M. E. Crestoni, D. Scuderi, R. K. Sinha, P. Maitre, and S. Fornarini, *Inorg. Chem.* **50** (2011) 4445−4452.
47. J. A. Wyer, A. V. Jørgensen, B. Møller Pedersen, and S. Brøndsted Nielsen, *ChemPhysChem* **14** (2013) 4109−4113.
48. J. A. Wyer and S. Brøndsted Nielsen, *Angew. Chem. Int. Ed.* **51** (2012) 10256−10260.